A high performance photonic pulse processing device

David Rosenbluth[2], Konstantin Kravtsov[1], Mable P. Fok[1], and Paul R. Prucnal[1]*

[1]*Princeton University, Princeton, New Jersey 08544, U.S.A.*
[2]*Lockheed Martin Advanced Technologies Laboratory, Cherry Hill, New Jersey, 08002, U.S.A.*
**prucnal@princeton.edu*

Abstract: This paper presents an all optical fiber based implementation of a hybrid analog-digital computational primitive that provides a basis for complex processing on high bandwidth signals. A natural implementation of a hybrid analog/digital photonic processing primitive is achieved through the integration of new nonlinear fiber, and exploitation of the physics of semiconductor device to process signals in unique ways. Specifically, we describe the use of a semiconductor optical amplifier to implement leaky temporal integration of a signal and a highly Ge-doped nonlinear fiber for thresholding. A straightforward correspondence between our computational primitive and leaky-integrate-and-fire neurons permits leveraging of a large body of research characterizing the computational capabilities of these devices and the emerging pulse processing computational paradigm as a means to implement practical signal processing algorithms in hybrid computing platforms. An experimental demonstration of the behavior of the pulse processing primitive is presented.

OCIS codes: (200.3050) Information processing; (190.4360) Nonlinear optics, devices; (200.4700) Optical neural systems.

References and links

1. C. Koch, Biophysics of Computation (Oxford University Press, 1999).
2. Y. Abu-Mostafa, and D. Psaltis, "Optical neural computers (invited)," Sci. Am. **256**, 88–95 (1987).
3. S. Jutamulia, and F. T. S. Yu, "Overview of hybrid optical neural networks," Opt. Laser Technol. **28**(2), 59–72 (1996).
4. M. T. Hill, E. E. E. Frietman, H. de Waardt, G. D. Khoe, and H. S. Dorren, "All fiber-optic neural network using coupled SOA based ring lasers," IEEE Trans. Neural Netw. **13**(6), 1504–1513 (2002).
5. R. Sarpeshkar, "Analog versus digital: extrapolating from electronics to neurobiology," Neural Comput. **10**(7), 1601–1638 (1998).
6. W. Maass, and C. M. Bishop, eds., Pulsed Neural Networks (The MIT Press, 1999).
7. M. Premaratne, D. Neˇsi'c, and G. P. Agrawal, "Pulse amplification and gain recovery in semiconductor optical amplifiers: A systematic analytical approach," J. Lightwave Technol. **26**(12), 1653–1660 (2008).
8. K. Kravtsov, P. R. Prucnal, and M. M. Bubnov, "Simple nonlinear interferometer-based all-optical thresholder and its applications for optical CDMA," Opt. Express **15**(20), 13114–13122 (2007).
9. E. M. Dianov, and V. M. Mashinsky, "Germania-based core optical fibers," J. Lightwave Technol. **23**(11), 3500–3508 (2005).

1. Introduction

In this paper we present a photonic computational primitive which operates at TeraHertz rates and can overcome both the scaling problems of digital optical computation, and the noise accumulation problems of analog optical computation. Our approach combines the picosecond processing and switching capabilities of both linear and nonlinear optical device technologies to integrate both analog and digital optical processing into a single hardware architecture capable of ultra fast computation without the need for A/D conversion. With this hybrid analog/digital processing primitive, it will be possible to implement processing algorithms of

#116749 - $15.00 USD Received 3 Sep 2009; accepted 23 Nov 2009; published 30 Nov 2009

far greater complexity than is possible with existing optical technologies, and far higher bandwidth than is possible with existing electronic technologies.

The design and implementation of our device is based upon a well-studied and paradigmatic example of a hybrid computational primitive: the spiking neuron. These simple computational elements integrate a small set of basic operations (delay, weighting, spatial summation, temporal integration, and thresholding) into a single device which is capable of performing a variety of computations depending on how its parameters are configured (e.g., delays, weights, integration time constant, threshold). The leaky-integrate-and-fire (LIF) neuron model is an abstraction of the spiking neurons which predominate animal nervous systems, and is well-established as the most widely used model of biological neurons in theoretical neuroscience for studying complex computation in nervous systems [1]. LIF neurons have recently attracted the attention of engineers and computer scientists for the following reasons:

- Algorithmic Expressiveness: They provide a powerful and efficient computational primitive from the standpoint of computational complexity and computability theory;
- Hardware Efficiency/Robustness: They are both robust and efficient processing elements. Complex algorithms can be implemented with less hardware;
- Utility in signal processing: There are known pulse processing algorithms for complex signal processing tasks (drawn from neuro-ethology). Pulse processing is already being used for implementing robust sensory processing algorithms in analog VLSI.

The photonic computational primitive presented in this paper is the first all optical implementation of a spiking LIF neuron. Due to its hybrid analog/digital nature it is capable of overcoming both the noise problems of purely analog optical devices and the limited computational capabilities of purely digital optical devices. Optical implementations of neural computation have been of interest for many years. Freespace optical devices (lenses, spatial filters, holograms) have been exploited for their ability to efficiently weight, spatially sum, and distribute signals with a high degree of parallelism [2,3]. However, freespace optical computations are limited to linear transforms. Previous fiber based implementations of neural computation have been limited to purely analog, approaches using semiconductor optical amplifier's which are prone to noise accumulation and instability when cascaded [4].

In the following we present: the overall architecture and operation of the photonic pulse processing primitive; a discussion of each of the device components of the architecture with emphasis on the use of an Semiconductor Optical Amplifier (SOA) as a leaky integrator; mapping between equations describing SOA gain dynamics and the equations prescribing the integration of LIF neurons is presented which validates SOA device physics as an embodiment of a leaky integrator; and experimental results showing the integrate-and-fire operation of a prototype photonic neuron.

2. Spike Process in a Neuron and the Matching with SOA Gain Dynamic

The functional architecture of the integrate and fire device (Fig. 1) consists of three processing blocks: (i) passive weighting, delay, and summation of inputs; (ii) temporal integration; and (iii) thresholding. A key finding is an *exact* correspondence between the equations governing SOA carrier density and the equations governing leaky integration in LIF neuron models, which justifies the use of an SOA as the embodiment of the leaky integrator in the computational primitive.

#116749 - $15.00 USD Received 3 Sep 2009; accepted 23 Nov 2009; published 30 Nov 2009

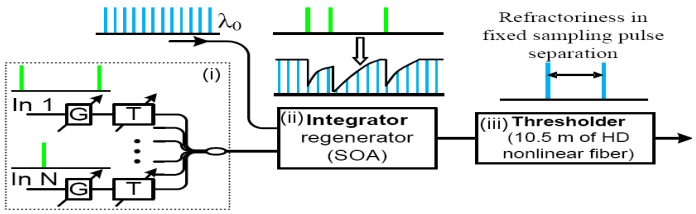

Fig. 1. Block diagram of the photonic neuron. G: gain; T: time delay; SOA semiconductor optical amplifier: HD nonlinear fiber: highly Ge-doped nonlinear fiber. The three processing are (i) passive weighting, delay, and summation of inputs; (ii) temporal integration; and (iii) thresholding.

Spike processing is a hybrid of analog and digital processing that has evolved in biological (nervous systems) and engineered (neuromorphic analog VLSI) systems as a means to exploit the efficiency of analog computation while overcoming problem of noise accumulation inherent in analog computation [5]. In contrast to the traditional neural networks models in which neuron output is represented as an analog value, the output of a spiking neuron is binary; a spike is either present or absent, with no information present in the shape or amplitude of a spike. Spike processing uses the timing of spikes as the primary means of encoding information. In systems with high temporal resolution and relatively low amplitude resolution, this use of the high capacity timing channel is preferable. Spike processing algorithms are well understood in a number of important biological sensory processing systems and are finding growing use in signal processing applications [6]. From the standpoint of computability and complexity theory, integrate-and fire neurons are powerful computational primitives that are capable of simulating both Turing machines and traditional neural networks [6].

The standard LIF model of a neuron operates as follows [6]: A neuron has N inputs which are continuous time series consisting either of spikes or continuous analog values representing voltages; each input is independently weighted and delayed; the N weighted and delayed time series are spatially summed (summed pointwise); the resulting single time series is then temporally integrated using an exponentially decaying impulse response function; if the temporally integrated signal $V_m(t)$ exceeds a threshold, then the neuron outputs a spike; after issuing a spike, there is a short period of time, the refractory period, during which no other spikes can be issued. The output of the neuron consists of a continuous time series consisting of spikes. The parameters determining the behavior of the device are: the weights ω_i, delays δ_i, threshold V_{thresh}, resting potential V_{rest}, refractory period $T_{refract}$, and the integration time constant τ_m that determines the exponential decay rate of the impulse response function for temporal integration.

Equations (1) and 2 below show the remarkable correspondence between the electrical model of leaky integration of membrane voltage and the optical model of SOA carrier density. Biological neurons are electrical devices, with membrane voltage, V_m, the primary internal state variable. There are three influences on V_m: passive leakage of current; an active pumping current; and external inputs generating time varying membrane conductance changes $\sigma(t)$. These three influences are the three terms contributing to the differential equation describing V_m in Eq. (1) below.

$$\underset{\text{Activation}}{\frac{dV_m(t)}{dt}} = \underset{\text{Active pumping}}{\frac{V_{\text{rest}}}{\tau_m}} - \underset{\text{Leakage}}{\frac{V_m(t)}{\tau_m}} - \underset{\text{External input}}{\frac{1}{C_m}V_m(t)\sigma(t)} \qquad (1)$$

$$\frac{dN'(t)}{dt} = \frac{N'_{\text{rest}}}{\tau_e} - \frac{N'(t)}{\tau_e} - \frac{\Gamma a}{E_p}N'(t)I(t) \qquad (2)$$

Equation (2) describes the gain dynamics of a short SOA when input pulse widths are much shorter than the carrier lifetime [7]. The primary state variable for the SOA is carrier density above transparency $N'(t) = N(t) - N_0$ where $N(t)$ is actual carrier density and N_0 is carrier density

#116749 - $15.00 USD Received 3 Sep 2009; accepted 23 Nov 2009; published 30 Nov 2009

at transparency. The integrative properties of the SOA are determined by: carrier lifetime τ_e; mode confinement factor Γ; differential gain coefficient a; photon energy E_p; and the active SOA pumping current. Spontaneous carrier decay tends to drive N' toward 0. An active pumping current is needed to counter the carrier decay and maintain a resting carrier density of N'_{rest}. Therefore, there are three contributions to $N'(t)$: a leakage term due to passive carrier decay; a term for carrier density due to active optical pumping of the SOA; and a term for carriers generated by external inputs. Due to the direct mapping of the electrical model of membrane voltage and the optical model of SOA carrier density, SOA device physics can be used as the analog implementation of a leaky integrator in our optical implementation of the LIF neuron.

3. Experimental Implementation of a Complete Neuron

The optical implementation of a complete neuron is described in Fig. 2. The input block consists of an N:1 optical coupler with a variable attenuator and a variable delay line in each of the inputs; the temporal integration block consists of an SOA with a gain sampling mechanism; the thresholding block consisting of an EDFA followed by an fiber based thresholder.

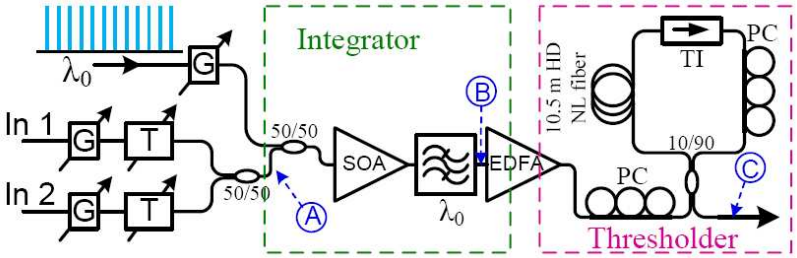

Fig. 2. Experimental setup. G: variable attenuator, T: variable delay line, PC: polarization controller, TI: tunable isolator [8], EDFA: erbium-doped fiber amplifier.

Our experimental realization of a neuron has two inputs with independent delay and attenuation controls. The diagram does not show auxiliary devices such as supplementary electronics, optical pulse sources and modulators. As a master pulse source a 1.25 GHz mode-locked ring fiber laser (MLL) is used. To provide pulse trains at multiple wavelengths, a supercontinuum generator with spectral slicing is utilized. The resulting width of optical pulses is about 3 ps FWHM. Mach-Zehnder optical modulators and a standard bit error tester were used for creating different pulse patterns required in performed measurements. The output resulted from passive weighting, delay, and summation of inputs is indicated as (A) in Fig. 2. The combined inputs are integrated at the SOA that changes the magnitude of SOA carrier density. In order for the magnitude of SOA carrier density to be used as an input to later stages of processing, it must be converted into a pulse intensity magnitude. Gain sampling is used as the means of converting SOA carrier density to pulse intensity. A low energy external pulse train from a MLL at wavelength λ_0, different from the wavelengths of the input signal, provides a sampling input to the SOA. Since the energy of the sampling pulses is small, their effect on the SOA gain is negligible in comparison to the effect of the input signals. As both the sampling pulses and the input signal pass through the SOA simultaneously, the amplification of the sampling pulses provides a measure of SOA carrier density primarily affected by the input signals. A band-pass spectral filter at the SOA output passes only the sampling pulses to the thresholder. This process regenerates the optical signal since it is the sampling pulse train, rather than transformed input signals, that is the output of the integrator as indicated as (B) in Fig. 2. Due to the utilized mechanism of integration with SOA gain sampling, the result of the thresholding, indicated as (C) is the absence of a spike when inputs exceed the threshold, and the presence of spikes when input is below threshold. Since this is inverted with respect to the

#116749 - $15.00 USD Received 3 Sep 2009; accepted 23 Nov 2009; published 30 Nov 2009

output of the integrate-and-fire model, an additional inversion step is required. Inverting the output is straightforward using e.g. an XOR gate.

To experimentally demonstrate the integration properties of the SOA with gain sampling, we excited the neuron with a series of input pulses while scanning the SOA gain with weaker sampling pulses. The results of the measurement are shown in Fig. 3. The gain dynamics of the SOA in response to input signals can be measured through its effect on the amplification of sampling signals. Figure 3(b) shows the input signal amplitude vs. time. Figure 3(a) shows the energy of the sampling pulses after passing through the SOA with the input pulses, using the same time scale as Fig. 3(b). The "resting potential", i.e. the maximum SOA gain when no control signal is present, was equal to 43 fJ. The measurements show: each input pulse leads to a decrease in energy of sampling pulses due to cross-gain modulation (XGM) in the SOA; the power of sampling pulses gradually increases as SOA gain recovers; and a series of input pulses creates a saw-tooth-like sample pulse intensity curve indicative of SOA gain recovery and the associated temporal integration properties of the SOA. The integration time constant, i.e. the SOA carrier lifetime τ_e, can be adjusted in the range from 100 to 300 ps by changing the SOA pump current. In this measurement τ_e = 180 ps.

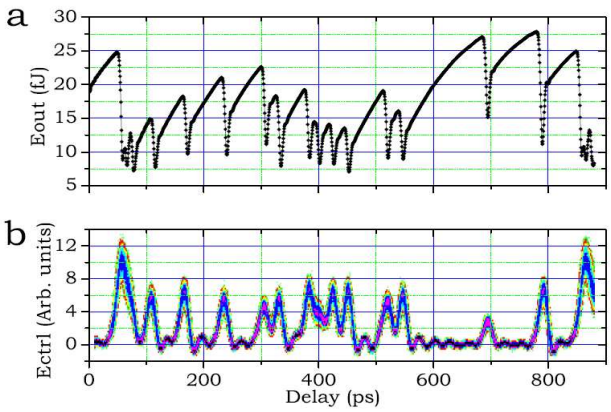

Fig. 3. The measured SOA response to excitation by multiple pulses. (a) Sampled SOA gain dynamics; (b) Oscilloscope trace of the control pulse sequence. The SOA recovery time (integration time constant) is 180 ps, resting potential level equals 43 fJ.

The last element of the LIF neuron is the thresholding mechanism. We use a nonlinear-fiber-based all optical thresholder based on a modified nonlinear optical loop mirror [8]. The thresholder contains 10.5 m of a heavily GeO_2-doped (HD) ([9], preform 311) with fiber parameters measured at λ = 1550 nm: nonlinear coefficient 35 $W^{-1}km^{-1}$, propagation losses 36 dB/km, chromatic dispersion −70 ps/nm km, refractive index difference $\Delta n = 0.11$. In order to effectively use the thresholder, which has a cubic transfer function saturating at higher powers [8], its input power is controlled by adjusting the gain in the EDFA directly preceding the thresholder.

An example of the thresholder operation in the neuron is shown in Fig. 4. In this experiment, both neuron inputs were connected to a source generating a digital 5- bit pattern '01100'. These inputs were weighted equally, and one input was delayed by approximately 1 bit, before summing. The weighted, delayed, and summed signals measured at the integrator input (point A in 1 was therefore '01210', as shown in part A of Fig. 4. The integrator output (point B on the block diagram), shown in part B of Fig. 4, contains pulses of three different heights: the highest corresponds to no input pulses, the middle — to one pulse, and the lowest — to both pulses present at the input. Depending on the gain setting of the EDFA preceding the thresholder, the neuron can discriminate between the lowest and the middle pulse energies or between the

#116749 - $15.00 USD Received 3 Sep 2009; accepted 23 Nov 2009; published 30 Nov 2009

middle and the highest. Both possibilities were experimentally demonstrated in the current setup with the corresponding measurements shown in Fig. 4. Also two trivial cases of thresholding with the threshold below the smallest pulse energy and above the highest were realized. The thresholder is capable of clear separation between ‘a pulse’ and ‘no pulse’ at its output depending on the threshold.

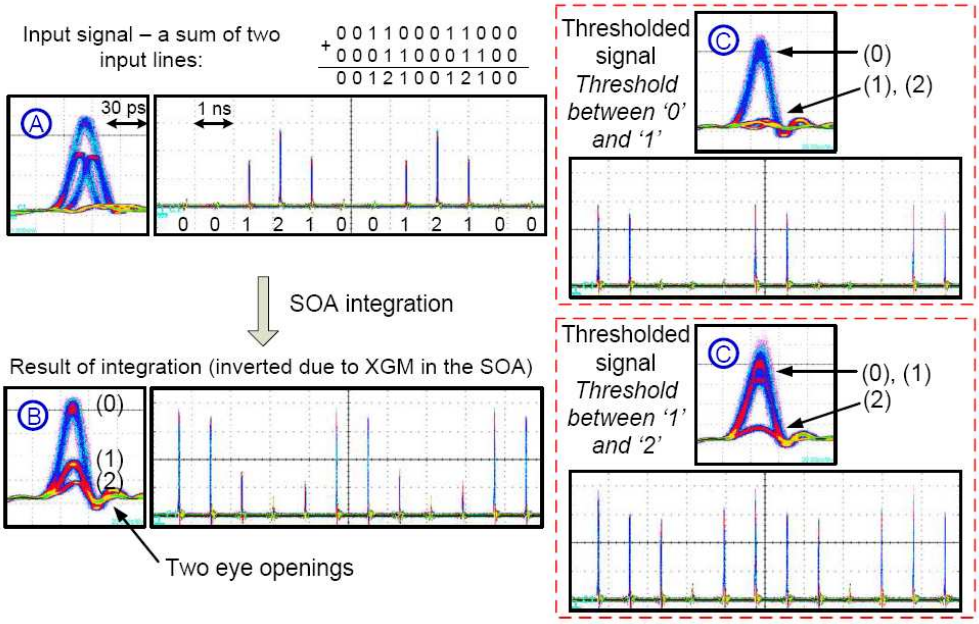

Fig. 4. An experimental demonstration of the all-optical thresholder operation. A — the measured input signal, which is a sum of two pulse streams; B — the integrator output; C — the thesholded signal, measured at two different threshold positions.

4. Conclusion

The spike processing device presented is an all-optical realization of the integrate-and-fire neuron model. The experimentally demonstrated integrate-and-fire device operates on picosec width pulses, and has an integration time constant of 180 ps, which can be also adjusted within the range from 100 to 300 ps. Reconfiguration of device parameters enables it to perform a wide variety of signal processing and decision operations. Its analog properties make it well suited to efficient signal processing applications, while its digital properties make it possible to implement complex computations without excessive noise accumulation. There is a straightforward mapping from traditional neural networks to spiking neural network which opens a range of potential new all-optical processing capabilities.

Acknowledgment

This work was supported by the Lockheed Martin Advanced Technology Laboratory.

#116749 - $15.00 USD Received 3 Sep 2009; accepted 23 Nov 2009; published 30 Nov 2009